Journal of Structural Biology 191 (2015) 49–58

Contents lists available at ScienceDirect

Journal of Structural Biology

journal homepage: www.elsevier.com/locate/yjsbi

High throughput screening using acoustic droplet ejection to combine protein crystals and chemical libraries on crystallization plates at high density

Ella Teplitsky [a,c,1], Karan Joshi [a,d,1], Daniel L. Ericson [a,e], Alexander Scalia [a,f], Jeffrey D. Mullen [a,g], Robert M. Sweet [b], Alexei S. Soares [b,*]

[a] Office of Educational Programs, Brookhaven National Laboratory, Upton, NY 11973-5000, USA
[b] Photon Sciences Directorate, Brookhaven National Laboratory, Upton, NY 11973-5000, USA
[c] Department of Biochemistry and Cell Biology, Stony Brook University, NY 11794-5215, USA
[d] Department of Electronics and Electrical Communication Engineering, PEC University of Technology, Chandigarh, India
[e] Department of Biomedical Engineering, University at Buffalo, SUNY, 12 Capen Hall, Buffalo, NY 14260, USA
[f] Department of Biological Sciences, 4400 Vestal Parkway East, Binghamton University, NY 13902, USA
[g] Physics Department, University of Oregon, Eugene, OR 97403-1274, USA

ARTICLE INFO

Article history:
Received 8 August 2014
Received in revised form 21 May 2015
Accepted 27 May 2015
Available online 29 May 2015

Keywords:
High throughput screening
Fragment screening
Drug discovery
Chemical biology
Acoustic droplet ejection
In situ X-ray data collection
Crystallography
Synchrotron radiation

ABSTRACT

We describe a high throughput method for screening up to 1728 distinct chemicals with protein crystals on a single microplate. Acoustic droplet ejection (ADE) was used to co-position 2.5 nL of protein, precipitant, and chemicals on a MiTeGen *in situ-1* crystallization plate™ for screening by co-crystallization or soaking. ADE-transferred droplets follow a precise trajectory which allows all components to be transferred through small apertures in the microplate lid. The apertures were large enough for 2.5 nL droplets to pass through them, but small enough so that they did not disrupt the internal environment created by the mother liquor. Using this system, thermolysin and trypsin crystals were efficiently screened for binding to a heavy-metal mini-library. Fluorescence and X-ray diffraction were used to confirm that each chemical in the heavy-metal library was correctly paired with the intended protein crystal. A fragment mini-library was screened to observe two known lysozyme ligands using both co-crystallization and soaking. A similar approach was used to identify multiple, novel thaumatin binding sites for ascorbic acid. This technology pushes towards a faster, automated, and more flexible strategy for high throughput screening of chemical libraries (such as fragment libraries) using as little as 2.5 nL of each component.
© 2015 The Authors. Published by Elsevier Inc. This is an open access article under the CC BY-NC-ND license (http://creativecommons.org/licenses/by-nc-nd/4.0/).

1. Introduction

High throughput screening using X-ray crystallography is a powerful tool for applications such as fragment library screening (for structure-based drug discovery) and additive library screening (for improving crystal quality) (Spurlino, 2011). For structure-based drug discovery projects (Blundell et al., 2002) the screened library may consist of individual fragments (Chilingaryan et al., 2012) or pooled fragments (Nicholls et al., 2010). For crystal quality improvement projects the screened library may contain additives such as protic ionic liquids (Kennedy et al., 2011). The chemicals being screened can be added either before crystal formation (co-crystallization) or after the crystals have grown (soaking). With either method, the objective is to screen a library which may consist of several thousand chemicals using a minimum amount of purified protein, screened chemicals, and other consumables.

Acoustic droplet ejection (ADE) has a demonstrated utility for growing protein crystals (Villasenor et al., 2012), improving the quality of protein crystals (Villasenor et al., 2010), mounting protein crystals onto data collection media (Soares et al., 2011; Roessler et al., 2013), and for high throughput screening of protein crystals (Yin et al., 2014). ADE uses a sound pulse (Fig. 1) to propel a liquid or suspended solid out of a source location, through a short air column, and onto an arbitrary destination (Ellson et al., 2003; volume accuracy 5%, trajectory precision 1.3°). The high trajectory precision enables "drop on drop" combination of distinct components from different source wells onto the same destination

* Corresponding author.
E-mail address: soares@bnl.gov (A.S. Soares).
[1] The two co-first authors contributed equally to this work.

http://dx.doi.org/10.1016/j.jsb.2015.05.006
1047-8477/© 2015 The Authors. Published by Elsevier Inc.
This is an open access article under the CC BY-NC-ND license (http://creativecommons.org/licenses/by-nc-nd/4.0/).

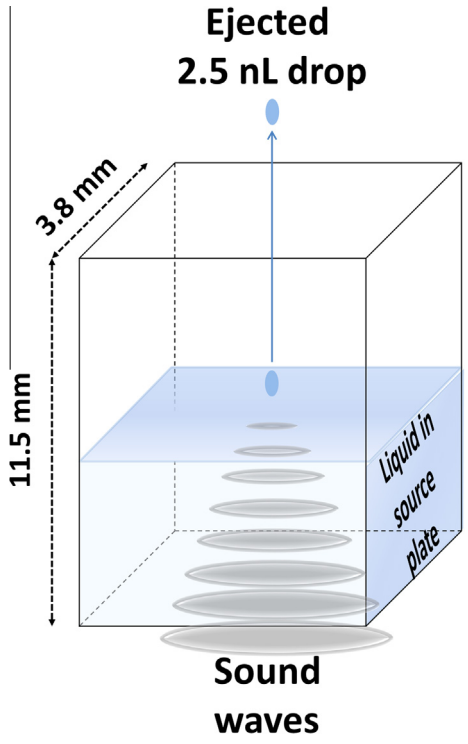

Fig. 1. Acoustic droplet ejection. ADE uses sound energy to transfer variable micro-droplets (e.g. nanoliter or picoliter) of solution (protein, precipitant, chemicals, etc.) from a well in a source plate through a short air column (~1 cm) to data collection media. Sound wave energy from the transducer is channeled to the focal point (i.e. ejection zone) displacing the surface where a controlled ejection occurs. Droplet size is governed by the wavelength of the sound emitted. In this work an Echo 550 was used to combine proteins, precipitants, and chemicals for co-crystallization and soaking experiments in 1728 distinct locations on a MiTeGen *in situ* crystallization plate. The Echo 550 does not use frequency changes to transfer different volumes. Instead, it uses a fixed frequency sound pulse to transfer each component in 2.5 nL increments.

location. The trajectory precision is sustained across a wide variety of commercially available crystallization conditions and cryo-protectants (Cuttitta et al., 2015). The Echo 550 acoustic liquid handler used in this study (Labcyte Inc., Sunnyvale, CA) transfers liquids using increments of 2.5 nL (ejection velocity ~1 m/s).

Villasenor and co-authors have suggested that acoustic methods might be used for structure-based drug discovery by co-crystallizing protein and fragments using a shared reservoir on a conventional crystallization plate (Villasenor et al., 2012, 899¶6). Note that this strategy employs the same precipitant to drive crystallization in all 96 wells of the crystallization microplate. Acoustic methods are an attractive choice for micro-crystallization for several reasons. ADE is an automated technique that does not rely on operator skill. It is physically gentle with no tips or tubes that may leach chemicals, cause cross-contamination between specimens (McDonald et al., 2008), or damage crystals. Transfers have high accuracy even at very low volume (2.5 nL) with zero per transfer "lost volume" since there are no tips or tubes that liquids can adhere to. The inaccessible "dead volume" at the bottom of each well is very small (4 μL; Harris et al., 2008) and can be reduced even further (Cuttitta et al., 2015). Specimen transfer is fast (500 mounts per second between fixed locations; 2.33 ± 0.04 mounts per second to multiple destinations, data not shown), which reduces specimen preparation time. Our system for room temperature fragment library screening is keyboard controlled and remote compatible, and can be readily mastered by new users.

As the working volume for crystallization drops below ~50 nL, dehydration becomes the foremost challenge. Our group made a previous attempt to develop the on-plate high throughput screening technology proposed by Villasenor et al. in 2012 without success (and we know of other similar attempts by other groups from personal communications). We tried several strategies for mitigating the impact of dehydration, such as working at 4 °C, parsing big jobs into small pieces, or simply working faster. None of these mitigation strategies were sufficient when dealing with 2.5 nL working volumes. To reduce dehydration we transferred all protein, precipitant and fragment components through small apertures in a plate lid that covered the MiTeGen *in situ-1* crystallization plate™ (Zipper et al., 2014). The MiTeGen plate was allowed to equilibrate with the precipitant before the crystallization fluids were ejected onto it (Fig. 2). A separately designed custom plate lid was used to cover the source plate (that contained the mini-libraries) to prevent the dimethyl sulfoxide (DMSO) that was solvating the chemicals from swelling with incorporated water when exposed to atmospheric humidity.

Here we describe a high throughput technique for screening protein crystals against a chemical library, using ADE to prepare co-crystallization or soaking experiments on MiTeGen crystallization microplates (Fig. 3). A critical advantage of ADE is that it can deposit solutions at their intended destination with a very high positional accuracy. The capability to combine protein, precipitant, and screened chemicals at 1728 distinct locations on a MiTeGen crystallization microplate is one advantage of this positional accuracy that we have already mentioned. Since the precise location of each of these 1728 experiments is known, there is also the opportunity to automate the data acquisition process by programming the plate-handling system (such as the G-rob system used in this work) to rapidly move between the 1728 known specimen locations. *In situ* data can then be obtained under computer control so that high throughput screening can occur without operator assistance. The speed and automation of this data acquisition approach could facilitate structure-based, high throughput fragment screening without grouping chemicals into cocktails. This mitigates the harmful effects of a high aggregate fragment concentration on protein stability and crystallization (Boyd and de Kloe, 2010; Baurin et al., 2004), prevents inter-fragment interactions (Drinkwater et al., 2010; Nair et al., 2012), and avoids the need to de-convolute the fragments in each cocktail after a hit (Nicholls et al., 2010).

2. Methods

We used two techniques for high throughput screening of proteins against chemical libraries, using X-ray crystallography as the primary screening tool:

Co-crystallization of protein with a library of chemicals: DMSO-solvated libraries were co-crystallized with protein and screened *in situ* (Fig. 4A). The library chemicals were acoustically deposited on the crystallization plate before any other components were added, and the DMSO was allowed to evaporate (leaving the dry residue of the chemical)[2]. The reservoir was then filled with mother liquor and the crystallization plate was sealed with a custom fabricated plate lid (Fig. 2) (Zipper et al., 2014). Once the

[2] DMSO is widely used as a solvent for chemical libraries because it is polar (with properties similar to water) but it is aprotic (which extends the useful life of the chemicals in the library). However, DMSO is a protein denaturant that is poorly tolerated by many crystals (Arakawa et al., 2007). It is often desirable to remove the DMSO immediately before each chemical is combined with proteins. In our experiments DMSO could be removed by allowing the DMSO solvent to evaporate before the protein and precipitant were added (on top of the dry residue containing the chemical). Of course, this approach is only practical when screening non-volatile chemicals.

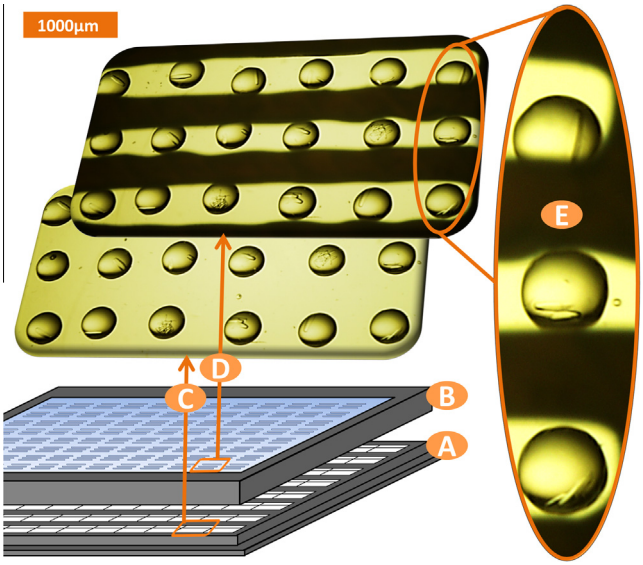

Fig. 2. Very small volumes of protein and chemicals can be used if all components are added through small apertures in otherwise-sealed containers. Thermolysin protein and chemicals were acoustically transferred to the crystallization plate (A) through apertures in the plate lid (B) to prevent the small volumes from drying (except for the DMSO that solvates library chemicals, which can be allowed to dry in a co-crystallization experiment). This prevents evaporation of the specimen (typically 2.5 nL of protein and chemical) while still allowing a high density of distinct experiments to share each crystallization well. MiTeGen crystallization plates, shown with the plate lid removed (C) and with the plate lid in place (D), can accommodate 3 rows and 6 columns of distinct co-crystallization or soaking screening experiments (18 screens per well and 96 wells make 1728 total screens per plate). Crystals can be seen through the apertures in the close up (E).

crystallization plate was equilibrated to the reservoir, acoustic methods were used to separately add protein and precipitant to 18 distinct locations in each of the 96 wells (1728 total experiments per microplate). Acoustic transfers were made through apertures in the crystallization plate lid, so that the crystallization plate was equilibrated to the mother liquor before, during, and after the addition of all components (except for DMSO-solvated chemicals, which were intentionally allowed to dry).

Soaking of proteins with a library of chemicals: Soaking experiments were similar, but the library chemicals were separately added to each of the 1728 locations on the MiTeGen plate after the crystals had formed (Fig. 4B). In this strategy, crystals were grown by vapor diffusion (by adding protein and precipitant to the 1728 locations), and the library chemicals were added afterwards. Each chemical was allowed to soak with the protein crystal for 1 h before data collection. In soaking experiments, it was not possible to prevent the DMSO from contacting the protein. Consequently, soaking experiments used water to solvate the chemicals in our mini-libraries instead of DMSO.

Each of the 96 crystallization wells in a MiTeGen *in situ-1* crystallization plate™ accommodated up to 18 co-crystallization or soaking experiments; these 1728 distinct specimens (each containing similar protein crystals and a different chemical) were then screened *in situ* using a plate handling system (le Maire et al., 2011). A very high density of specimens could share a single crystallization plate, making the experiment compact. The number of distinct experiments that can be accommodated on one MiTeGen plate is equivalent to 13½ Dewars, each fully loaded with 8 V1 uni-pucks. A very high rate of sustained data acquisition was possible, using the plate handling system to rapidly move between specimen locations (see Section 2.5).

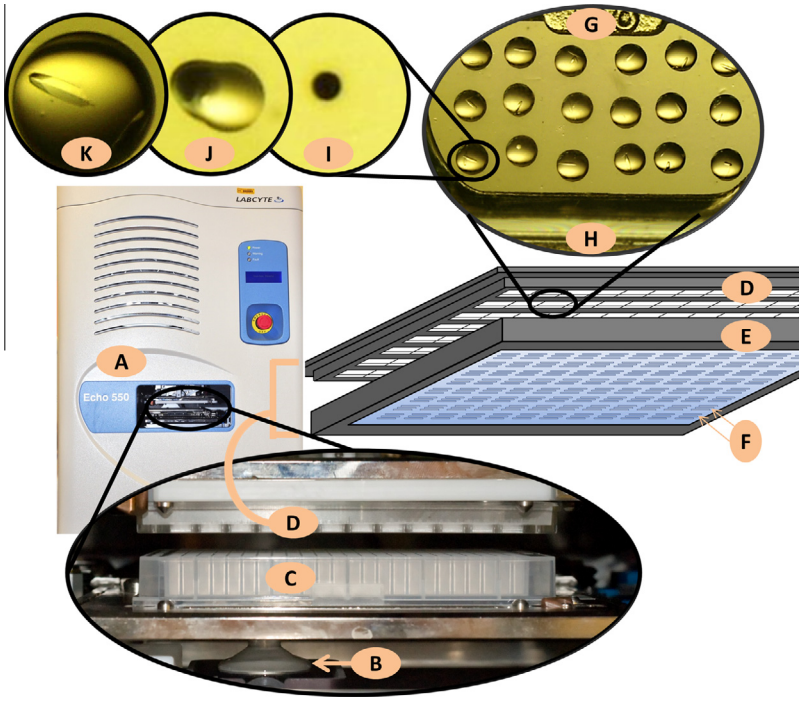

Fig. 3. Using acoustic droplet ejection (ADE) to screen 1728 chemicals on one MiTeGen crystallization microplate. The Echo 550 (A) uses sound energy to transfer microdroplets of protein, precipitant, or chemical from a library (typically a fragment library). A motorized transducer (B) moves under the source plate (C) to the location of each building block in the experiment and generates a sound pulse that ejects 2.5 nL onto a MiTeGen *in situ-1* crystallization plate™ ((D), shown without plate lid for clarity). The crystallization plate is sealed by a plate lid (E) which contains small apertures (F) through which each component is transferred to the crystallization region (G). The precipitant in the reservoir (H) governs the humidity of the plate before, during, and after protein transfer. In a co-crystallization experiment, DMSO-solvated screened chemicals are often added to the crystallization plate before the reservoir is filled (with no plate lid) and the DMSO is allowed to evaporate, leaving behind the dry chemical residue (I). The plate is then sealed by the plate lid and equilibrated with the reservoir. Protein and precipitant (J) are added through the apertures and combined with each screened chemical. Vapor diffusion drives co-crystallization (K) of the protein and each screened chemical. Soaking experiments are prepared in a similar way, but screened chemicals are added after the crystals have grown.

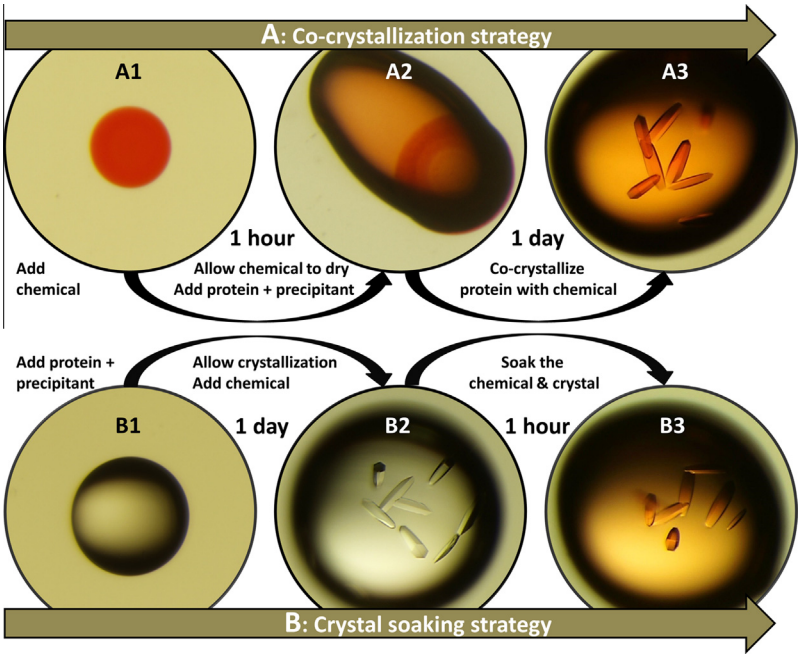

Fig. 4. Both co-crystallization and soaking strategies are possible for high throughput screening of high-density fragment libraries deposited on crystallization microplates (thermolysin crystals are shown with eosin colorant). *Co-crystallization:* High throughput screening of protein crystals and a fragment library using co-crystallization (A) uses ADE to deposit 2.5 nL of each DMSO-solvated chemical fragment at each distinct location on the crystallization plate (1728 locations per MiTeGen plate) (A1). Each DMSO-solvated fragment is allowed to dry for 1 h. The crystallization plate is then sealed with a plate lid (Fig. 2) and equilibrated with the protein precipitant solution. ADE is then used to add protein and precipitant, through apertures, on top of the dry residue from each fragment in the library (A2). Vapor diffusion drives co-crystallization of each fragment and protein over 24 h (A3). *In situ* data collection is recorded from the crystals in each droplet. *Soaking:* High throughput screening of protein crystals and a fragment library by soaking each fragment with a crystal (B) uses ADE to deposit protein and precipitant at each distinct location in a sealed crystallization plate that is equilibrated with the protein precipitant (B1). Vapor diffusion drives crystallization over 24 h (B2). Each chemical fragment is then soaked into a different protein crystal for 1 h (B3) and X-ray diffraction data is obtained from each crystal/fragment soak.

A plate-specific definition that allows the *Echo Array Maker* software (Labcyte Inc., Sunnyvale, CA) to operate the Echo 550 and dispense liquids to 18 locations in each of the 96 crystallization wells on a MiTeGen plate is available from our group on request. This plate definition was made in two stages using *Echo Array Maker*. First, an array definition was generated to access each of the 96 wells on the MiTeGen plate. Then, the software was used to further partition each crystallization well into 3 rows by 6 columns of accessible destination locations using 1000 μm grid spacing.

To demonstrate the Echo 550s capability to prepare specimens in MiTeGen plates, we first used conventional manual techniques to verify reliable crystallization conditions for four test proteins (lysozyme, thermolysin, trypsin, and thaumatin) using the conventional hanging drop vapor diffusion method (Table 1). For each protein, the same crystallization conditions identified in the manual experiments were found to be effective in the acoustically prepared experiments (with the working volume reduced 100 0-fold). In our experiments the precipitant in the reservoir was held in place by a 1% agarose solution (Whon et al., 2009).

Diffraction data were collected at the National Synchrotron Light Source (NSLS) beamlines X12b and X25. Data sets were processed with *HKL2000* (Otwinowski and Minor, 2001) and further processed using *CTRUNCATE* in the CCP4i suite (Winn et al., 2011). Structures were obtained by molecular substitution from published models and refined using *REFMAC* (Winn et al., 2003) and *ArpWarp* (Perrakis et al., 2001) (starting models 1lyz-lysozyme, 4tln-thermolysin, 4i8 g-trypsin, 1thi-thaumatin) (Diamond, 1974; Holmes and Matthews, 1981; Liebschner et al., 2013; Kim et al., 1988). Binding fragments were identified in a $F_{obs} - F_{calc}$ omit difference map by visual inspection using *coot* (Emsley and Cowtan, 2004).

2.1. Using methylene blue to probe for cross-contamination

Compact specimen holders such as the high-density MiTeGen microplates described here can accelerate applications such as fragment screening. Our objective was to maximize the number of specimens that can be discretely assembled on a MiTeGen plate without cross-contamination between adjacent experiments. However, as the density of specimens is increased there is the danger that adjacent experiments will become cross-contaminated. To test the capability of the Echo 550 to accurately dispense building blocks to 18 distinct locations in each MiTeGen crystallization well, we alternately dispensed colored (methylene blue colorant) and clear droplets to form a checkerboard pattern at nearly twice the specimen density as we used in our experiments (32 locations per well compared to 18 locations) (Fig. 5). The blue dye used in this demonstration imparts a distinctive color even at 1% concentration, so that even very limited cross-contamination could be easily detected by visual inspection.

2.2. Screening a heavy-metal mini-library by soaking

In addition to preventing cross-contamination, compact high-density formats for high throughput screening must reliably deliver each screened chemical to the desired location. To verify the fidelity of our strategy for delivering screened chemicals, we assembled a mini-library of 6 heavy-metals. The soaking strategy (Fig. 4B) was used for this demonstration, so each heavy-metal solution was added to already-grown thermolysin and trypsin crystals. Excitation scans were then used to detect the presence of each heavy atom by recording the fluorescence peak at the expected X-ray wavelength. The excitation scans were performed

Table 1
Crystallization conditions.

	Lysozyme	Trypsin	Thermolysin	Thaumatin
Protein	120 mg/mL	30 mg/mL + 10 mg/mL benzamidine	330 mg/mL + 45% DMSO	50 mg/mL
Buffer	0.1 M NaAc pH4.6	10 mM $CaCl_2$ + 20 mM HEPES pH 7	50 mM tris pH 7.5	Distilled water
Precipitant	8% NaCl	40% PEG 8000 + 400 mM $AmSO_4$ + 200 mM bis–tris	1.45 M $CaCl_2$	1.5 M NaK tartrate + 0.1 M bis–tris propane pH 6.6

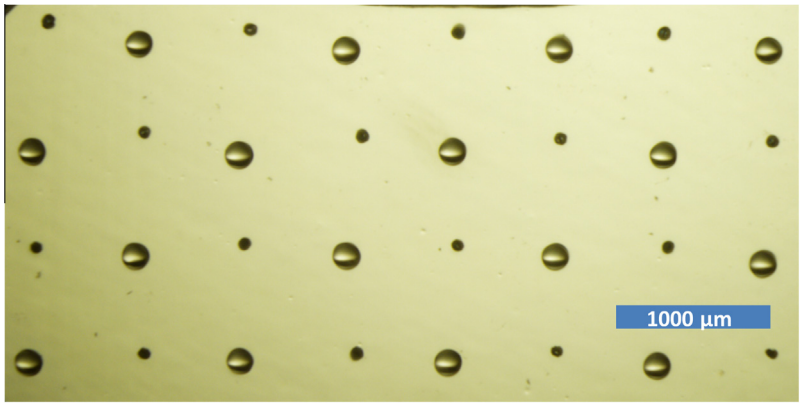

Fig. 5. Highly accurate droplet transfers prevent cross-contamination. A checkerboard pattern of highly concentrated blue dye (methylene blue) was alternated with a 50/50 mixture of water and DMSO (clear solvent). The methylene blue was solvated in water and dehydrated almost instantly (leaving the dark residue shown), while the DMSO-containing drops remained hydrated (because DMSO is hygroscopic). The methylene blue is an intense pigment that is evident at low concentration (a 100-fold dilution of the starting concentration is still blue and easy to see), so even a modest amount of cross-contamination should be evident. The field of view shown here contains 32 equally spaced droplets at moderate magnification. We carefully examined 12 similar fields under high magnification (a total of 384 distinct droplets). None of the examined fields contained any evidence of cross-contamination. The largest positional error for all of the 384 droplets tested was less than half of the target distance between the droplets. Given that the specimen density shown here is almost twice the specimen density that we used in our experiments, we conclude that the likelihood of cross-contamination with our high throughput screening strategy is very small.

using a G-rob plate-screening robot to discretely target each of the 18 separate crystal containing droplets that had been soaked with six heavy-metal solutions. Each heavy-metal was soaked into the crystals on three droplets in each of the six columns. This way, the MiTeGen plate well contained three similar rows, each of which contained the same sequence of heavy-metals.

2.3. Screening a mini-library for known lysozyme ligands

Lysozyme crystals were soaked and co-crystallized with a fragment mini-library. Previous groups have described data collection from one or several protein crystals that reside in a crystallization microplate well and which share a similar chemical environment (Axford et al., 2012). We obtained *in situ* data from 18 lysozyme crystals residing in a crystallization microplate well, with each crystal having a unique chemical environment (each drop contained the same precipitant and protein, but a different screened chemical). We used both co-crystallization and soaking approaches to combine lysozyme crystals with an 18-chemical fragment mini-library in a single well of a crystallization microplate (in total this experiment occupied eight crystallization wells). We then separately obtained *in situ* data from each of the 18 different fragment chemicals. Our fragment mini-library contained benzamidine (Table 2) and N-acetyl glucosamine, which are known lysozyme ligands. We searched for the known ligands by inspecting the electron density map.

2.4. Screening a high concentration library with thaumatin in situ

We determined micro-crystallization conditions that commonly yield exactly one protein crystal in each 25 nL thaumatin vapor diffusion crystal growth screen (Table 1). We prepared a mini-library of 36 safe laboratory chemicals at high concentration (100–500 mM). Some of the mini-library chemicals were not sufficiently soluble to form 100 mM solutions; in these cases the excess chemical remained as a suspended solid (this includes the ascorbic acid solution which is further described in Section 3.4). We then grew thaumatin crystals on the same material that is used in MiTeGen plates. Some of the crystals were grown on conventional MiTeGen *in situ-1* plates (at a density of 18 distinct crystallization droplets per crystallization well), and some of the crystals were grown in a custom crystallization chamber that contains 36 distinct crystallization droplets per crystallization well (the custom crystallization chamber is compatible with conventional magnetic pins, similar to the sample mounting grid described in Cohen et al., 2014; currently under patent review). Each crystallization droplet (usually containing exactly one crystal) was then combined with one chemical from the mini-library, and allowed to soak for 1 h (including solutions containing suspended solids). X-ray diffraction data were then obtained from one crystal in each crystallization droplet.

2.5. In situ screening and diffraction data collection

The G-rob plate screening system at NSLS X12b was a convenient high throughput tool for screening chemical libraries at room temperature *in situ* on crystallization plates. The system includes a customizable interface for partitioning each MiTeGen crystal well into N by M discreet targets of equal size (N and M are integers). Using the CBASS data acquisition software (Skinner et al., 2006), we could automatically move to each of the 18 locations on each of the 96 crystallization wells in the MiTeGen plates. Each target could also be automatically photographed with the in-line camera. By pairing the automated data collection protocol with known crystal locations, we tested automatic screening of 1728 experiments. However, technical difficulties (see discussion) limited the achieved autonomy to 18–36 specimens. Consequently, we used the G-rob plate screening system only to screen the heavy metals

(Section 2.2) and approximately 20% of the ligands (Section 2.4). The remaining ligands were screened at room temperature *in situ* at X25. The bromine binding to trypsin (protein data bank 4TPY) and the ascorbic acid binding to thaumatin (protein data bank 4TVT) that we observed in our room-temperature experiments (see Sections 3.2 and 3.4) were repeated at X25 with similarly prepared specimens that were cryo-cooled (two last columns in Table 2).

Because mechanical problems limited the automation potential for the G-rob, we developed a strategy for obtaining *in situ* data at NSLS X25 (a more powerful beamline). Since no plate handling system is available at X25, we mechanically cut our MiTeGen plates into plate pieces small enough to be secured onto a conventional goniometer head (Soares et al., 2014). This yielded improved data by matching the low mosaic spread of our room temperature crystals with the fast readout speed of the Pilatus 6M detector at X25. In this way, we could overcome the reduced signal that is available from the low X-ray dose limits for room temperature crystals by reducing the background noise using a fine phi slicing strategy (0.1°) that exploited the low mosaicity (~0.04°) of our room temperature crystals (Owen et al., 2014). Approximately 80% of the electron density maps in this project were obtained from X25 using plate pieces, or using the custom crystallization chamber mentioned in Section 2.4. Since lysozyme, trypsin, and thaumatin crystals have similar diffraction limit (~1.2 Å) and mosaicity (~0.04°), we used a similar data collection strategy for all of these crystals (0.1° rotation, 0.1 s exposure, ~220 mm detector distance, 10× attenuation, 50 μ beam). Although optimal data would have been obtained from even smaller oscillations (1/2 mosaicity ≈ 0.02°, see Mueller et al., 2011), data collection time would have been prohibitive.

3. Results

Our strategy was to exploit the reduced mosaicity of room temperature crystals to support a 0.1° fine phi slicing data collection strategy. In this way we compensated for the low dose-tolerance of the room temperature crystals by using fine phi slicing to reduce the background noise. In favorable cases, the low mosaicity of room temperature crystals yielded signal-to-noise ratios comparable to those of cryo-cooled crystals.

3.1. Preventing cross-contamination

To ensure that the three-by-six specimen deposition density would segregate the contents of adjacent experiments, we deposited alternating clear droplets and droplets containing methylene blue at a density of droplets that was almost double that used in our experiments (32 versus 18 droplets per crystallization well). A representative picture of a high-density field is shown in Fig. 5. Visual inspection of 12 equivalent high-density fields showed that cross-contamination did not occur in any of the 384 repetitions. The methylene blue dye used in this experiment is clearly visible even at 1% concentration so we are confident that any cross-contamination would have been evident by inspection.

3.2. Heavy-metal mini-library soaked into thermolysin and trypsin crystals

As positive controls, we soaked six readily detectable heavy-metal reagents with crystals of thermolysin and trypsin. A picture of one row of six crystals that were soaked with six heavy-metal reagents has been rotated by 90° for clarity (Fig. 6, column 2). A close-up view of the crystals in the picture is also shown (column 3). We used a G-rob plate-handling system to separately probe each of the 18 soaking experiments for the presence of the expected heavy-atom. In all 18 cases we positively identified the expected heavy-atom in each location by observing a fluorescence peak at the appropriate wavelength for each heavy-atom (Fig. 6, column 4). We also obtained room temperature X-ray diffraction data from thermolysin and trypsin crystals that were soaked with each of the six heavy-metal solutions. For each of these twelve data sets (both proteins soaked with six metals each), representative reflections with a common resolution of ~2.3 Å were picked from the last frame of the data collection sweep. These reflections showed that the cumulative X-ray dose did not

Table 2
Data collection and model refinement statistics (dose was estimated using RADDOSE, see Zeldin et al., 2013).

Protein	Lysozyme (RT)		Thaumatin (RT)	Trypsin (RT)	Thaumatin (100 K)	Trypsin (100 K)
Ligand	Benzamidine (co-cr.)	Benzamidine (soak)	Ascorbic acid	Sodium bromide	Ascorbic acid	Sodium bromide
Data collection statistics						
X-ray source	NSLS X25			NSLS X12b	NSLS X25	
Focus FWHM (μm)	360 × 70			800 × 200	360 × 70	
Exposure time (s)	0.1			2.0	1.0	
Attenuation	0.1			1.0	1.0	
Wavelength (Å)	1.1	1.1	1.1	0.9198	1.1	0.9198
Detector dist. (mm)	220	220	220	120	200	200
Beam aperture (μm)	75 × 75	100 × 100	100 × 100	150 × 150	50 × 50	50 × 50
Image width (°)	0.1	0.1	0.1	0.2	1.0	1.0
Data wedge (°)	100	100	100	50	270	270
Average dose (MGy)	0.11	0.11	0.10	0.04	3.30	3.10
Crystal quality statistics						
Crystal size (mm)	100 × 100	100 × 100	120 × 120	200 × 1000	100 × 100	150 × 700
Refined mosaicity (°)	0.03	0.05	0.05	0.06	0.37	0.43
Resolution (Å)	1.2 (26.8)	1.4 (44.0)	1.2 (54.0)	1.3 (44.0)	1.2 (54.0)	1.3 (44.0)
$R_{sym\ (\%)}$	4.5 (16.9)	5.8 (31.2)	3.4 (68.5)	8.1 (84.1)	2.9 (34.7)	6.4 (42.5)
$I/\sigma I$	66.19 (11.5)	34.03 (3.7)	36.3 (1.0)	18.4 (0.8)	42.8 (1.0)	27.4 (1.1)
Completeness (%)	100.0 (100.0)	98.0 (90.1)	69.3 (31.6)	73.5 (41.7)	89.9 (23.6)	90.4 (33.2)
Redundancy	17.3	5.3	6.8	7.5	14.6	10.6
Modeling and refinement statistics						
No. of reflections	34,003	22,042	52,773	38,989	68,461	44,900
R_{work}/R_{free}	22.9/25.1	14.7/17.9	14.7/17.7	14.9/18.4	14.6/16.2	14.2/17.2
RMS bond length (Å)	0.029	0.028	0.031	0.023	0.034	0.025
RMS bond angles (°)	2.441	2.441	2.875	2.236	2.941	2.361

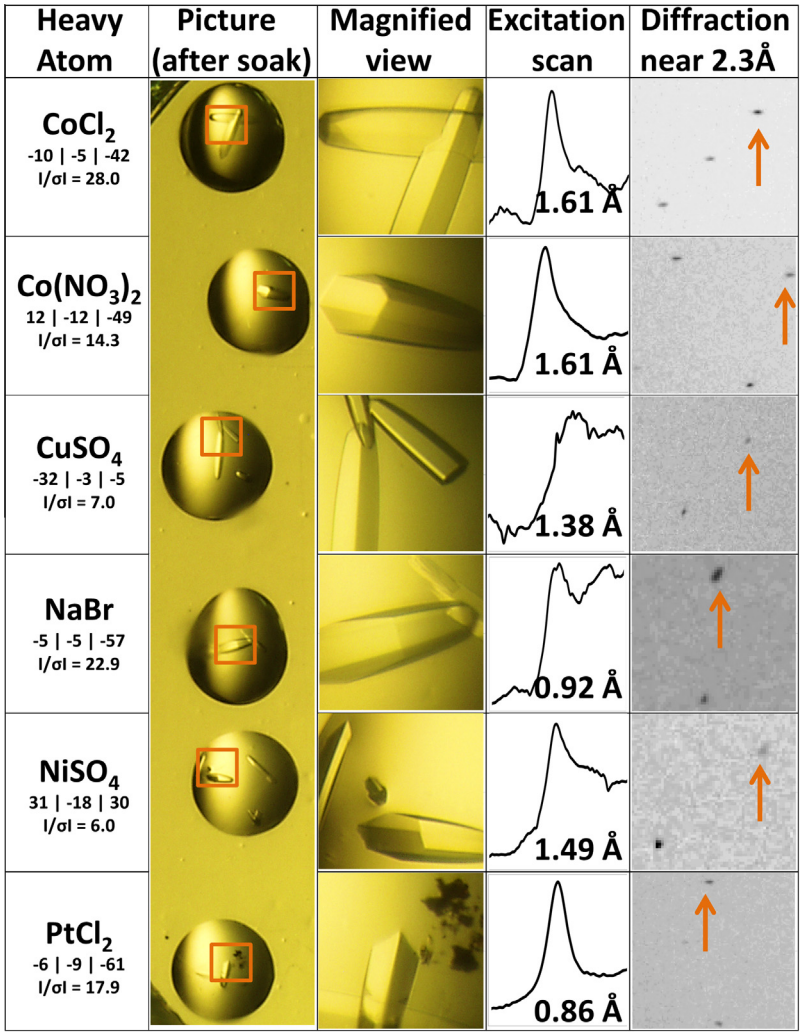

Fig. 6. Excitation scans were used to confirm that thermolysin crystals were successfully combined with six heavy-metal reagents. Column 1 contains the name of each heavy-metal reagent and information about the sample reflection indicated in column 5 (index and signal-to-noise). Column 2 is a single picture of six thermolysin crystals after soaking with the six heavy-metal reagents. Column 3 shows a magnified view of each crystal (the insoluble platinum compound can be seen in the bottom row). Column 4 shows the excitation scan at the white line (wavelength shown) for each heavy atom. Column 5 is a magnified view of a few reflections from the last frame of the data collection sweep, with resolution near 2.3 Å (the orange arrow indicates the reflection described in column 1).

excessively dim the diffraction power of the crystal (the index and signal-to-noise ratio for each reflection is shown in Fig. 6, column 1, along with a picture in column 5). The twelve thermolysin crystals diffracted to an average resolution of 1.9 ± 0.1 Å with an average mosaicity of 0.09 ± 0.03° (data not shown). The twelve trypsin crystals diffracted to an average resolution of 1.4 ± 0.2 Å with an average mosaicity of 0.06 ± 0.02°. Data collection and refinement statistics from the crystal where we first observed bromine bound to trypsin are shown in Table 2 (the other trypsin data sets that were obtained at X12b were similar).

We used excitation scans to confirm that trypsin crystals were successfully combined with the same six heavy-metal reagents that were used for thermolysin. All of the scans confirmed the presence of the desired heavy-atoms. We then obtained X-ray diffraction data from each of the crystals. All of the crystals diffracted to the typical resolution limit for trypsin. The data had anomalous signals for three known trypsin binding heavy-atoms (copper sulfate and the two cobalt salts had a strong anomalous signal, nickel sulfate had a weak anomalous signal).

The X-ray diffraction data also revealed anomalous signal for sodium bromide, a trypsin derivative that had not been previously deposited in the PDB. The structure of this derivative was readily solved [4TPY] using the anomalous diffraction from three high-occupancy bromine atoms (there are also lower occupancy sites). The phasing power was of high quality. Fig. 7 shows the experimental map ($F_{obs}\Phi_{obs}$, contoured at 2.5σ) superposed on the final atomic structure. The experimental map was generated from the anomalous data using *HKL2MAP* after 20 cycles of solvent flattening (Supplemental Fig. 1) (Pape and Schneider, 2004).

3.3. In situ ligand screening: known lysozyme ligands

We used both co-crystallization and soaking approaches to screen lysozyme crystals with a mini-library consisting of 18 chemicals (including the known ligands N-acetyl glucosamine and benzamidine). For both approaches, the resulting electron density confirmed that our library screening system had correctly paired the lysozyme crystals with its N-acetyl glucosamine ligand (data not shown) and with its benzamidine ligand (Fig. 8). None of the other 16 screened chemicals was observed in the electron density.

3.4. In situ fragment screening: novel thaumatin fragment hits

We soaked thaumatin crystals with a high-concentration mini-library (chemical concentrations were between 100 mM

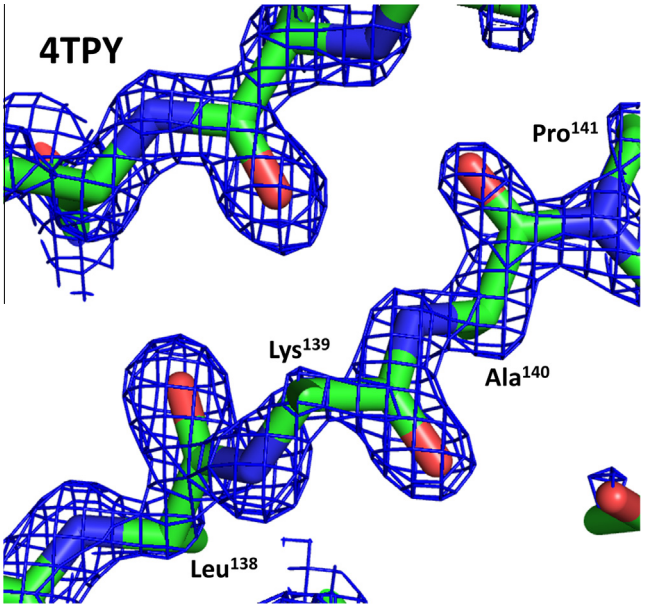

Fig. 7. We used excitation scans to confirm that trypsin crystals were successfully combined with the same six heavy-metal reagents that were used for thermolysin (the thermolysin data are in Fig. 6). All of the scans confirmed the presence of the desired heavy atom. We then obtained X-ray diffraction data from each of the crystals. All of the crystals diffracted to the typical resolution limit for trypsin. The data had anomalous signal for three known trypsin binding heavy-atoms (copper sulfate and the two cobalt salts had a strong anomalous signal, nickel sulfate had a weak anomalous signal). The X-ray diffraction data also revealed anomalous signal for sodium bromide, a trypsin derivative not previously deposited in the PDB. The structure of this derivative was readily solved [4TPY] using the anomalous diffraction from three bound bromine atoms. The phasing power was of high quality. The experimental map ($F_{obs}\Phi_{obs}$, contoured at 2.5σ) is superposed on the final atomic structure. The experimental map was improved by 20 cycles of solvent flattening.

and 500 mM). *In situ* data were obtained from either 18 or 36 separate crystals in each crystallization chamber, each soaked for 1 h with a different high concentration chemical from our mini-library. Using this strategy, we demonstrated that L-ascorbic acid binds to five locations on thaumatin. *In situ* data from thaumatin crystals soaked in 500 mM ascorbic acid revealed binding sites that were arranged into two clusters (Fig. 9). The ascorbic acid molecules in each cluster interacted with each other either directly (Panel B) or via bridging water molecules (Panel A).

4. Discussion

High throughput strategies that use X-ray diffraction to screen chemical libraries will benefit from improvements in technology that make better use of resources. We outline a strategy that uses acoustic specimen preparation with the Echo 550 to assemble 1728 distinct experiments on a MiTeGen microplate. Our strategy optimizes the use of resources such as space (1728 chemicals screened in one microplate), consumables (2.5 nL of protein, precipitant, and the screened chemical) and time (2.33 specimens prepared per second). By using the automated computer-controlled data collection strategy outlined in Section 2.5, our method also makes optimal use of synchrotron X-ray diffraction end stations which are limited in availability, and greatly minimizes the demand for scientific staff to supervise the data collection. Coupled with the brightness of 4th generation synchrotron sources such as NSLS II, our strategy will deliver unprecedented rates of data acquisition and a commensurately enhanced ability to screen large chemical libraries.

The most powerful high throughput screening capability of our system came from the integration of high throughput capabilities of the Echo 550 liquid handler and the G-rob plate-handling system. The combination of target location functionality of a liquid handler and automated plate handling system (which knows where to find each of the 1728 experiments) with the data collection software (which can obtain X-ray data under automated computer control), makes it possible to screen chemical libraries with an unprecedented level of automation. Since each crystal data set required about 20 min, the 1728 experiments in each MiTeGen microplate could hypothetically give this system an operational autonomy of 24 days. In practice, mechanical limitations restricted the achievable autonomy to just one or a few wells before the accumulation of target positioning errors caused the X-ray beam to begin missing the specimen. In part, these target positioning errors derive from a slight angular misalignment of the gripped plate (in one experiment, we measured a systematic 0.4° misalignment, so that each consecutive 9 mm well contributed 80 microns of error). Other factors may also contribute to random or systematic errors. Simple software improvements (such as coupling a short "grid scan" X-ray search protocol to a feedback loop) should prevent the buildup of positioning errors and allow fully automated screening of all 1728 experiments. Simple arithmetic demonstrates that this technology will allow the plate handling system at NSLS II to sustain a very high rate of data acquisition in high throughput screening applications.

Screening large fragment libraries for structure-based drug discovery projects will likely remain the most challenging mission for this type of high throughput screening. Libraries of this type can contain thousands of fragments. For these projects, we anticipate that our system will support a throughput rate for fragment screening that is greater than 1 data set per second. It can be challenging to obtain highly complete data from a single *in situ* crystal, so two or more data sets may be merged from

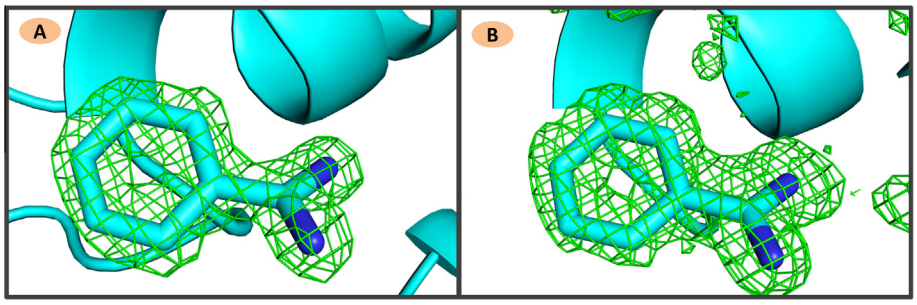

Fig. 8. *In situ* data collection identifies known lysozyme ligands from a fragment mini-library. We used a fragment mini-library with two known ligands of lysozyme to test our co-crystallization and soaking approaches for high throughput *in situ* screening. The omit difference electron density map for N-acetyl glucosamine (data not shown) and for benzamidine (shown above) revealed the known ligands (electron density contoured at 3σ) using both the crystal soaking strategy (panel A) and the co-crystallization strategy (panel B). For this experiment, we obtained *in situ* data from 18 protein crystals that reside in each microplate well (each crystal was combined with a different chemical at a concentration of 100 mM).

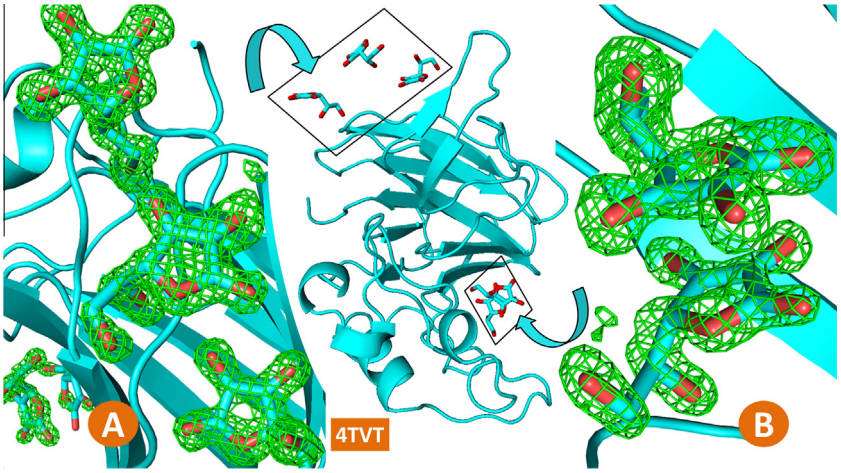

Fig. 9. *In situ* data collection identifies novel thaumatin ligands from a high-concentration fragment mini-library. High throughput screening using ADE reduces the use of protein and chemicals (2.5 nL used per screen), reduces the specimen preparation time (2.33 per second), reduces the consumption of labware (1728 screens per MiTeGen crystallization plate), and efficiently uses available synchrotron time (less down time for robotic specimen exchange). This efficient use of resources simplifies fragment screening using a "one at a time" strategy (without pooling different fragments into cocktails) at high concentrations (>100 mM) without the danger that a high aggregate chemical concentration may disrupt the integrity of the protein crystals. By screening a high concentration mini-library (500 mM) we identified multiple thaumatin binding sites for ascorbic acid [4TVT] (difference omit map shown in green). The binding sites were arranged into two clusters. The first cluster binds three ascorbic acid molecules (with end-to-end geometry) between two thaumatin proteins in adjacent asymmetric units (Panel A, contoured at $I/\sigma I = 3.0$). The second cluster binds two ascorbic acid molecules (with stacked ring geometry) in a cleft between the alpha-helical and beta-sheet domains of thaumatin (Panel B, contoured at $I/\sigma I = 2.0$). By facilitating the simultaneous observation of multiple copies of the same fragment (or of different fragments), this high-concentration strategy could elucidate ligand–ligand interactions (in addition to ligand–protein interactions). Information about ligand–ligand interactions might simplify the construction of tightly binding therapeutic compounds.

different crystals containing the same fragment (in some cases this may not be needed because fragment screening does not require high completeness, e.g. 71% in le Maire et al., 2011). For example, in the case of the NSLS II beamline AMX (which will be used to screen low mosaicity room temperature crystals), the maximum throughput speed will be limited by the detector readout rate (and not by the brilliance of the X-ray facility). For this example, if we optimistically project the medium term detector development outlook to a readout rate of 500 frames per second, then 0.1° data wedges will sample 50° of reciprocal space per second. This is approximately equal to the angular data acquisition limit for most *in situ* crystallization plates (including the MiTeGen plate; Soliman et al., 2011), so the screening throughput rate will be approximately one screened fragment per second. This is approximately equal to the time needed for a cryo-cooled 20 μm crystal to absorb an X-ray dose equal to the Henderson limit ($D_{1/4} = 10^7$ Gy, Henderson, 1990) at the AMX beamline (flux 10^{13} ph/s; Hodgson et al., 2009). At room temperature, the dose limit will be reduced by about 50-fold, so the X-ray beam will have to be attenuated in order to obtain a full data set from one crystal (unless much faster detectors become available). The crystal screening rate would still be limited by the detector speed and would remain approximately 1 screened chemical per second. Alternatively, the dose from the un-attenuated beam could be distributed by merging data from many crystals that all contain the same fragment.

The speed and flexibility of acoustic *in situ* high throughput screening will continue to advance with ongoing developments in robotic hardware, control software, and crystallization labware. We previously discussed the need to compensate for minor robotic drift and the potential to leverage advances in detector technology. Software could be back-integrated with the specimen preparation database and forward-integrated with tools for data collection, processing, and ligand search (Delagenière et al., 2011). Software support should also be expanded to other plate designs, such as the *Crystal Direct*™ plates. *Crystal Direct*™ plates have a very large crystallization shelf (we have accommodated 2016 specimens on one plate), and with the support of laser assisted crystal mounting systems (Cipriani et al., 2012) it should be possible to extend acoustic *in situ* technology to cryogenic specimens. New labware could also increase compatibility with beamlines that lack plate handling robots (Cohen et al., 2014). These improvements to acoustic *in situ* high throughput screening will continue to strengthen structure-based drug discovery as a mainstream tool to improve human health.

Acknowledgments

Personnel for this study were recruited largely through the 2014 spring session of the Science Undergraduate Laboratory Internships Program (SULI), supported through the U.S. Department of Energy, Office of Science, Office of Workforce Development for Teachers and Scientists (WDTS). Major ongoing financial support for acoustic droplet ejection applications was through the Brookhaven National Laboratory/U.S. Department of Energy, Laboratory Directed Research and Development Grant 11-008 and from the US Department of Energy Offices of Biological and Environmental Research and of Basic Energy Sciences grants DE-AC02-98CH10886 and DE-SC0012704 and from NIH grants P41-RR012408, P41-GM103473 and P41-GM111244. Data for this study were measured at beamlines X12b and X25 of the National Synchrotron Light Source. We thank Labcyte Inc., and especially Joe Olechno, Richard Ellson and Richard Stearns, for their technical support and guidance. Author contributions: A.S.S. designed the experiment and wrote the paper, with input from E.T. E.T., A.S.S., D.L.E., and A.S. grew crystals, obtained data and analyzed data. A.S.S., K.J., and J.D.M. designed and built the labware. A.S.S. and R.M.S. trained and supervised student interns.

Appendix A. Supplementary data

Supplementary data associated with this article can be found, in the online version, at http://dx.doi.org/10.1016/j.jsb.2015.05.006.

References

Arakawa, T., Kita, Y., Timasheff, S.N., 2007. Protein precipitation and denaturation by dimethyl sulfoxide. Biophys. Chem. 131 (1), 62–70.

Axford, D., Owen, R.L., Aishima, J., Foadi, J., Morgan, A.W., Robinson, J.I., Nettleship, J.E., Owens, R.J., Moraes, I., Fry, E.E., Grimes, J.M., Harlos, K., Kotecha, A., Ren, J., Sutton, G., Walter, T.S., Stuart, D.I., Evans, G., 2012. In situ macromolecular crystallography using microbeams. Acta Crystallogr. D Biol. Crystallogr. 68, 592–600.

Baurin, N., Aboul-Ela, F., Barril, X., Davis, B., Drysdale, M., Dymock, B., Finch, H., Fromont, C., Richardson, C., Simmonite, H., Hubbard, R.E., 2004. Design and characterization of libraries of molecular fragments for use in NMR screening against protein targets. J. Chem. Inf. Comput. Sci. 44, 2157–2166.

Blundell, T.L., Jhoti, H., Abell, C., 2002. High-throughput crystallography for lead discovery in drug design. Nat. Rev. Drug Discov. 1, 45–54.

Boyd, S.M., de Kloe, G.E., 2010. Fragment library design: efficiently hunting drugs in chemical space. Drug Discov. Today Technol. 7, e173–e180.

Chilingaryan, Z., Yin, Z., Oakley, A.J., 2012. Fragment-based screening by protein crystallography: successes and pitfalls. Int. J. Mol. Sci. 13, 12857–12879.

Cipriani, F., Rower, M., Landret, C., Zander, U., Felisaz, F., Marquez, J.A., 2012. CrystalDirect: a new method for automated crystal harvesting based on laser-induced photoablation of thin films. Acta Crystallogr. D Biol. Crystallogr. 68, 1393–1399.

Cohen, A.E., Soltis, S.M., González, A., Aguila, L., Alonso-Mori, R., Barnes, C.O., et al., 2014. Goniometer-based femtosecond crystallography with X-ray free electron lasers. Proc. Natl. Acad. Sci. USA 111 (48), 17122–17127.

Cuttitta, C.M., Ericson, D.L., Scalia, A., Roessler, C.G., Teplitsky, E., Joshi, K., Campos, O., Agarwal, R., Allaire, M., Orville, A.M., Sweet, R.M., Soares, A.S., 2015. A simple method for acoustically transferring protein crystals to X-ray data-collection media using agar pedestals. Acta Crystallogr. D Biol. Crystallogr. 71 (1), 94–103.

Delagenière, S., Brenchereau, P., Launer, L., Ashton, A.W., Leal, R., et al., 2011. ISPyB: an information management system for synchrotron macromolecular crystallography. Bioinformatics 27, 3186–3192.

Diamond, R., 1974. Real-space refinement of the structure of hen egg-white lysozyme. J. Mol. Biol. 82, 371–391.

Drinkwater, N., Vu, H., Lovell, K.M., Criscione, K.R., Collins, B.M., Prisinzano, T.E., Poulsen, S.A., McLeish, M.J., Grunewald, G.L., Martin, J.L., 2010. Fragment-based screening by X-ray crystallography, MS and isothermal titration calorimetry to identify PNMT (phenylethanolamine N-methyltransferase) inhibitors. Biochem. J. 431, 51–61.

Ellson, R., Mutz, M., Browning, B., Lee, L., Miller, M.F., Papen, R., 2003. Transfer of low nanoliter volumes between microplates using focused acoustics – automation considerations. J. Assoc. Lab. Autom. 8, 29–34.

Emsley, P., Cowtan, K., 2004. Coot: model-building tools for molecular graphics. Acta Crystallogr. D Biol. Crystallogr. 60, 2126–2132.

Harris, D., Mutz, M., Sonntag, M., Stearns, R., Shieh, J., Pickett, S., Olechno, J., 2008. Low nanoliter acoustic transfer of aqueous fluids with high precision and accuracy of volume transfer and positional placement. J. Assoc. Lab. Autom. 13, 97–102.

Henderson, R., 1990. Cryoprotection of protein crystals against radiation-damage in electron and X-ray-diffraction. Proc. R. Soc. London Ser. B. 241, 6–8.

Hodgson, K.O., Anderson, W.F., Berman, L.R., Fischetti, R., Hendrickson, W.A., Kirz, J., Makowski, L., Phillips, G.N., Smith, J.L., Sweet, R.M.., Tsuruta, H., 2009. Workshop of the National Institutes of Health National Center for Research Resources and the National Institute of General Medical Sciences on Plans for Support of Future Life Science Synchrotron Research at NSLS-II. Final Report, National Institutes of Health, Bethesda.

Holmes, M.A., Matthews, B.W., 1981. Binding of hydroxamic acid inhibitors to crystalline thermolysin suggests a pentacoordinate zinc intermediate in catalysis. Biochemistry 20, 6912–6920.

Kennedy, D.F., Drummond, C.J., Peat, T.S., Newman, J., 2011. Evaluating protic ionic liquids as protein crystallization additives. Cryst. Growth Des. 11, 1777–1785.

Kim, S.H., de Vos, A., Ogata, C., 1988. Crystal structures of two intensely sweet proteins. Trends Biochem. Sci. 13 (1), 13–15.

le Maire, A., Gelin, M., Pochet, S., Hoh, F., Pirocchi, M., Guichou, J.F., Ferrer, J.L., Labesse, G., 2011. In-plate protein crystallization, in situ ligand soaking and X-ray diffraction. Acta Crystallogr. D Biol. Crystallogr. 67, 747–755.

Liebschner, D., Dauter, M., Brzuszkiewicz, A., Dauter, Z., 2013. On the reproducibility of protein crystal structures: five atomic resolution structures of trypsin. Acta Crystallogr. D Biol. Crystallogr. 69, 1447–1462.

McDonald, G.R., Hudson, A.L., Dunn, S.M., You, H., Baker, G.B., Whittal, R.M., Martin, J.W., Jha, A., Edmondson, D.E., Holt, A., 2008. Bioactive contaminants leach from disposable laboratory plasticware. Science 322, 917.

Nair, P.C., Malde, A.K., Drinkwater, N., Mark, A.E., 2012. Missing fragments: detecting cooperative binding in fragment-based drug design. ACS Med. Chem. Lett. 3, 322–326.

Nicholls, A., McGaughey, G.B., Sheridan, R.P., Good, A.C., Warren, G., Mathieu, M., Muchmore, S.W., Brown, S.P., Grant, J.A., Haigh, J.A., Nevins, N., Jain, A.N., Kelley, B., 2010. Molecular shape and medicinal chemistry: a perspective. Journal of medicinal chemistry. J. Med. Chem. 53, 3862–3886.

Mueller, M., Wang, M., Schulze-Briese, C., 2011. Optimal fine-slicing for single-photon-counting pixel detectors. Acta Crystallogr. D Biol. Crystallogr. 68, 42–56.

Otwinowski, Z., Minor, W., 2001. Denzo and Scalepack. In: International Tables for Crystallography Volume F: Crystallography of Biological Macromolecules. Springer Netherlands, pp. 226–235.

Owen, R.L., Paterson, N., Axford, D., Aishima, J., Schulze-Briese, C., Ren, J., Fry, E.E., Stuart, D.I., Evans, G., 2014. Exploiting fast detectors to enter a new dimension in room-temperature crystallography. Acta Crystallogr. D Biol. Crystallogr. 70, 1248–1256.

Pape, T., Schneider, T.R., 2004. HKL2MAP: a graphical user interface for macromolecular phasing with SHELX programs. J. Appl. Crystallogr. 37, 843–844.

Perrakis, A., Harkiolaki, M., Wilson, K.S., Lamzin, V.S., 2001. ARP/wARP and molecular replacement. Acta Crystallogr. D Biol. Crystallogr. 57, 1445–1450.

Roessler, C.G., Kuczewski, A., Stearns, R., Ellson, R., Olechno, J., Orville, A.M., Allaire, M., Soares, A.S., Heroux, A., 2013. Acoustic methods for high-throughput protein crystal mounting at next-generation macromolecular crystallographic beamlines. J. Synchrotron Radiat. 20, 805–808.

Skinner, J.M., Cowan, M., Buono, R., Nolan, W., Bosshard, H., Robinson, H.H., Héroux, A., Soares, A.S., Schneider, D.K., Sweet, R.M., 2006. Integrated software for macromolecular crystallography synchrotron beamlines II: revision, robots and a database. Acta Crystallogr. D Biol. Crystallogr. 62, 1340–1347.

Soares, A.S., Engel, M.A., Stearns, R., Datwani, S., Olechno, J., Ellson, R., Skinner, J.M., Allaire, M., Orville, A.M., 2011. Acoustically mounted microcrystals yield high-resolution X-ray structures. Biochemistry 50, 4399–4401.

Soares, A.S., Mullen, J.D., Parekh, R., McCarthy, G.S., Roessler, C.G., Jackimowicz, R., Skinner, R., Orville, A.M., Allaire, M., Sweet, R., 2014. Solvent minimization induces preferential orientation and crystal clustering in serial micro-crystallography on micro-meshes, in situ plates and on a movable crystal conveyor belt. J. Synchrotron Radiat. 21, 6.

Spurlino, J.C., 2011. Fragment screening purely with protein crystallography. Methods Enzymol. 493, 321–356.

Soliman, A.S.M., Warkentin, M., Apker, B., Thorne, R.E., 2011. Development of high-performance X-ray transparent crystallization plates for in situ protein crystal screening and analysis. Acta Crystallogr. D Biol. Crystallogr. 67, 646–656.

Villasenor, A.G., Wong, A., Shao, A., Garg, A., Donohue, T.J., Kuglstatter, A., Harris, S.F., 2012. Nanolitre-scale crystallization using acoustic liquid-transfer technology. Acta Crystallogr. D Biol. Crystallogr. 68, 893–900.

Villasenor, A.G., Wong, A., Shao, A., Garg, A., Kuglstatter, A., Harris, S.F., 2010. Acoustic matrix microseeding: improving protein crystal growth with minimal chemical bias. Acta Crystallogr. D Biol. Crystallogr. 66, 568–576.

Whon, T.W., Lee, Y.H., An, D.S., Song, H.K., Kim, S.G., 2009. A simple technique to convert sitting-drop vapor diffusion into hanging-drop vapor diffusion by solidifying the reservoir solution with agarose. J. Appl. Crystallogr. 42, 975–976.

Winn, M.D., Ballard, C.C., Cowtan, K.D., Dodson, E.J., Emsley, P., Evans, P.R., Keegan, R.M., Krissinel, E.B., Leslie, A.G., McCoy, A., McNicholas, S.J., Murshudov, G.N., Pannu, N.S., Potterton, E.A., Powell, H.R., Read, R.J., Vagin, A., Wilson, K.S., 2011. Macromolecular TLS refinement in REFMAC at moderate resolutions. Methods in enzymology. Acta Crystallogr. D Biol. Crystallogr. 67, 235–242.

Winn, M.D., Murshudov, G.N., Papiz, M.Z., 2003. Macromolecular TLS refinement in REFMAC at moderate resolutions. Methods Enzymol. 374, 300–321.

Yin, X., Scalia, A., Leroy, L., Cuttitta, C.M., Polizzo, G.M., Ericson, D.L., Roessler, C.G., Campos, O., Ma, M.Y., Agarwal, R., Jackimowicz, R., Allaire, M., Orville, A.M., Sweet, R.M., Soares, A.S., 2014. Hitting the target: fragment screening with acoustic in situ co-crystallization of proteins plus fragment libraries on pin-mounted data-collection micromeshes. Acta Crystallogr. D Biol. Crystallogr. 70, 1177–1189.

Zeldin, O.B., Gerstel, M., Garman, E.F., 2013. RADDOSE-3D: time-and space-resolved modelling of dose in macromolecular crystallography. J. Appl. Crystallogr. 46, 1225–1230.

Zipper, L.E., Aristide, X., Bishop, D.P., Joshi, I., Kharzeev, J., Patel, K.B., Soares, A.S., 2014. A simple technique to reduce evaporation of crystallization droplets by using plate lids with apertures for adding liquids. Acta Crystallogr. F Struct. Biol. Commun. 70, 1707–1713.